Supporting Information

Four- and five-coordinate aluminum complexes supported by N,O-bidentate β-pyrazylenolate ligands: synthesis, structure and application in ROP of ε-caprolactone and lactide

Lu Qin,[a] Yue Zhang,[a] Jianbin Chao,[b] Jianhua Cheng,[c] Xia Chen*[a,c]

[a]School of Chemistry and Chemical Engineering, Shanxi University, Taiyuan, 030006, China.

[b]Scientific Instrument Center, Shanxi University, Taiyuan, 030006, China.

[c]State Key Laboratory of Polymer Physics and Chemistry, Changchun Institute of Applied Chemistry, Chinese Academy of Science, Changchun, 130022, China.

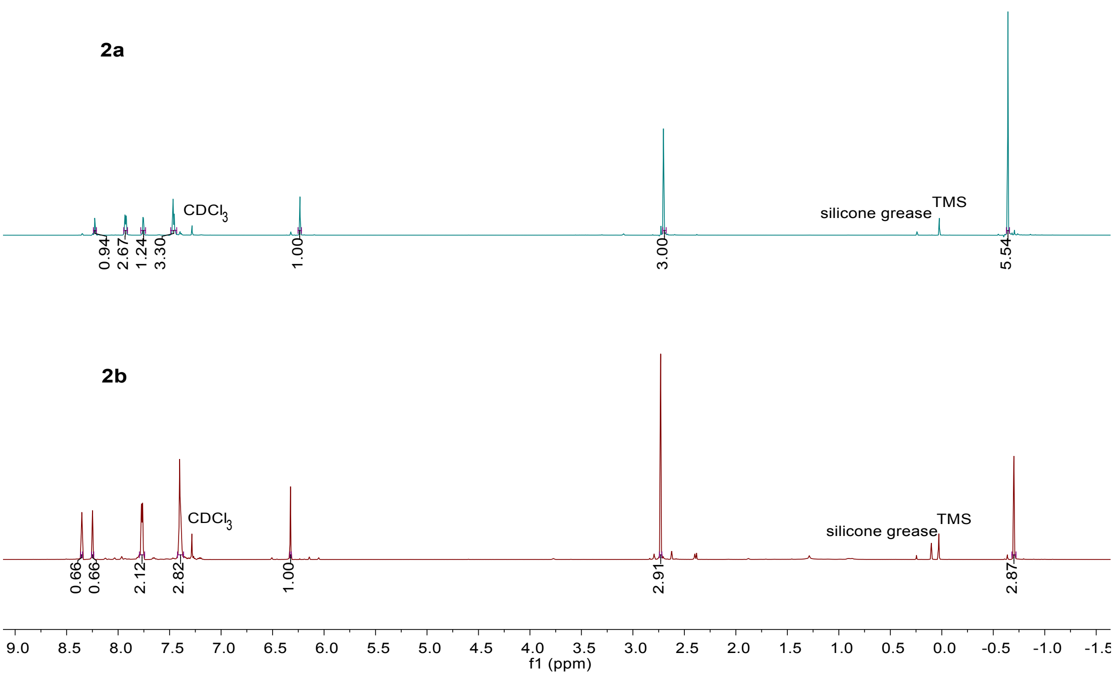

Figure S1 Comparison of ^{1}H NMR spectrums of **2a** and **2b** (600 MHz, $CDCl_3$, 25 °C)

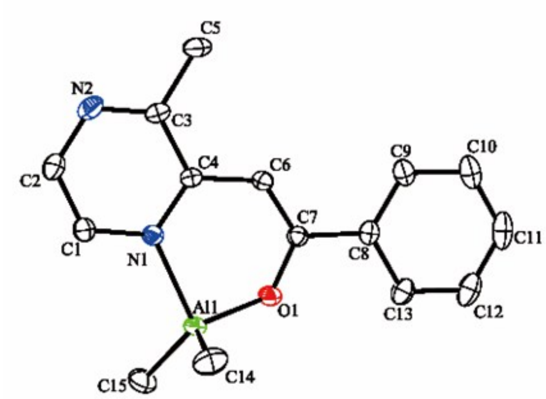

Figure S2 X-ray structure of **2a** with thermal ellipsoids represented at the 30% probability level. Hydrogen atoms are omitted for clarity.

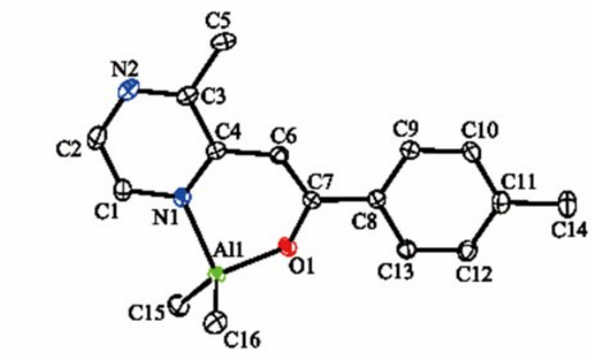

Figure S3 X-ray structure of **3a** with thermal ellipsoids represented at the 30% probability level. Hydrogen atoms are omitted for clarity.

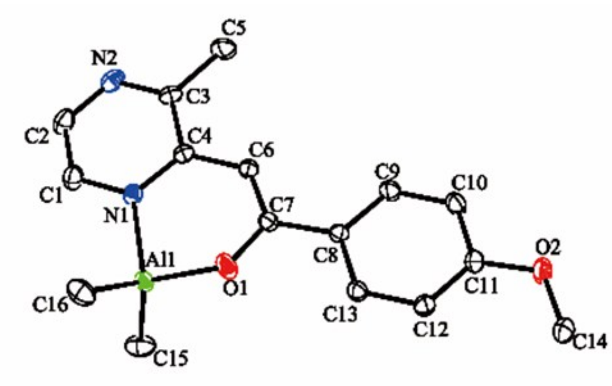

Figure S4 X-ray structure of **4a** with thermal ellipsoids represented at the 30% probability level. Hydrogen atoms are omitted for clarity.

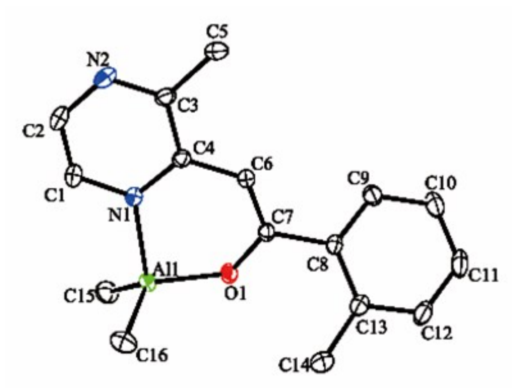

Figure S5 X-ray structure of **5a** with thermal ellipsoids represented at the 30% probability level. Hydrogen atoms are omitted for clarity.

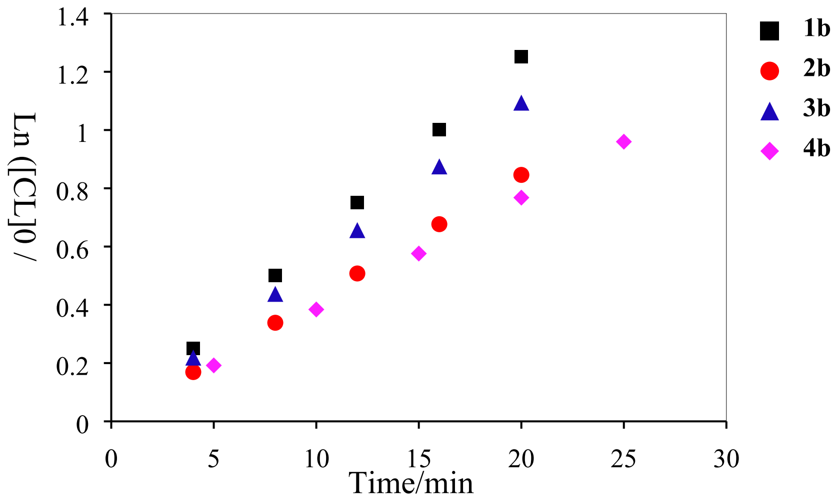

Figure S6 Relationship between ln([CL]$_0$/[CL]) and time of the polymerization initiated by **1b**–**4b** in the presence of BnOH in toluene at 50 °C with a ratio of [CL]$_0$:[Al]$_0$:[BnOH]$_0$ = 100:1:1 ([CL]$_0$ = 1 M).

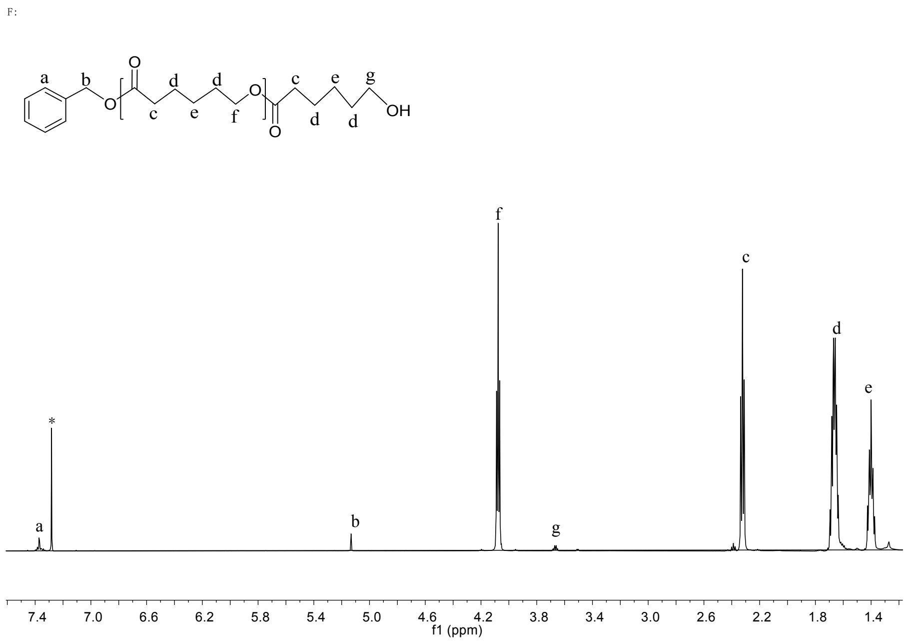

Figure S7 The ^{1}H NMR spectrum of PCL initiated by **1a**/BnOH in the ratio of [CL]$_0$:[Al]$_0$:[BnOH]$_0$ = 30:1:1 ([CL]$_0$ = 1 M) in toluene at 50 °C for 60 min.

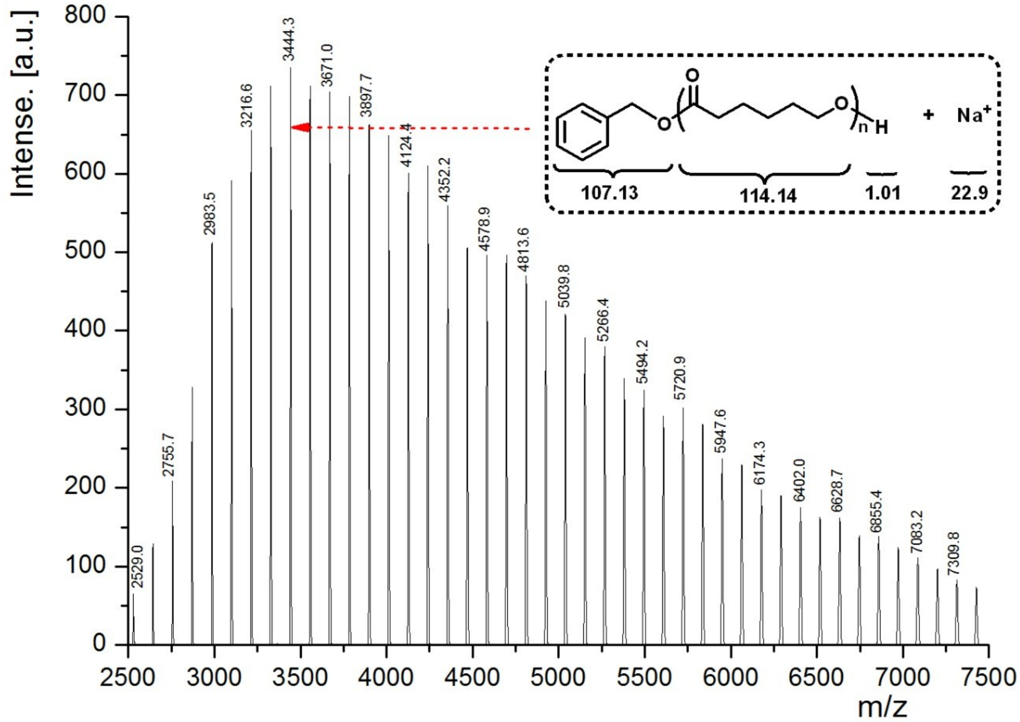

Figure S8 MALDI-TOF MS analysis for the resulting PCL produced by **5a** ($[CL]_0$:$[Al]_0$:$[BnOH]_0$ = 100:1:1, 50 ℃).

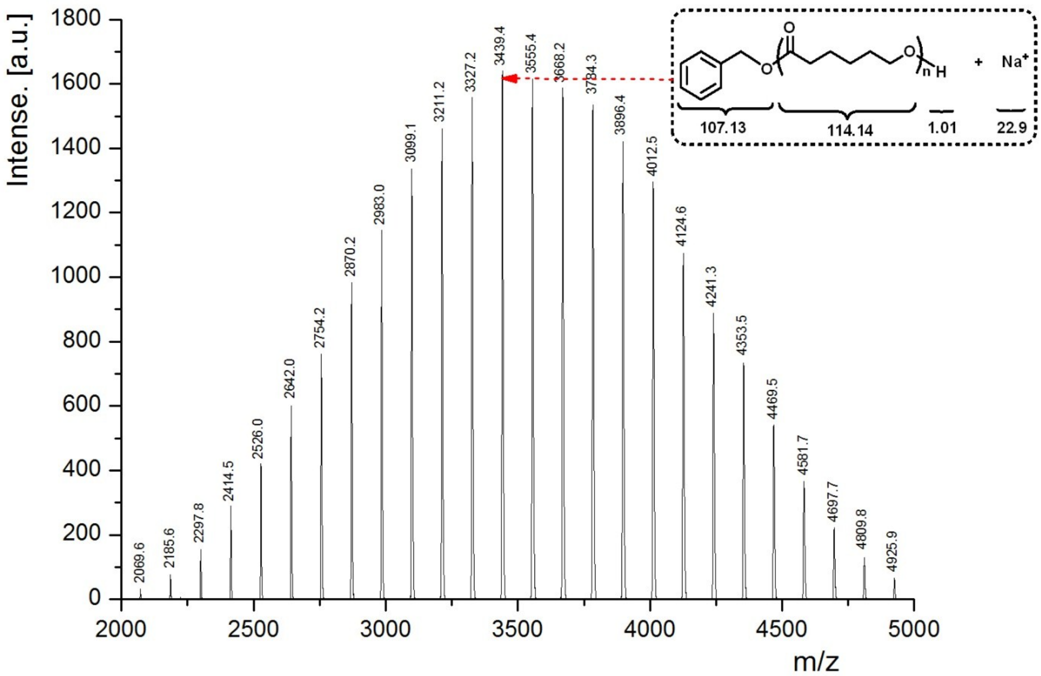

Figure S9 MALDI-TOF MS analysis for the resulting PCL produced by **5a** ($[CL]_0$:$[Al]_0$:$[BnOH]_0$ = 100:1:2, 50 ℃).

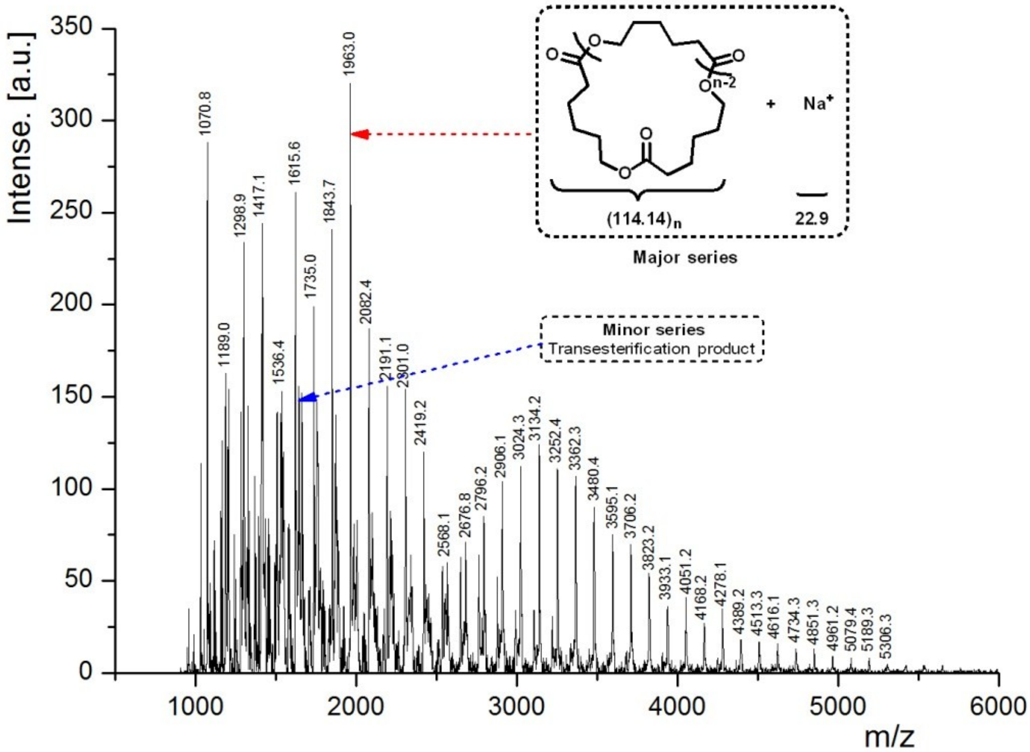

Figure S10 MALDI-TOF MS analysis for the resulting PCL produced by **5a** ($[CL]_0$:$[Al]_0$:$[BnOH]_0$ = 100:1:0, 50 ℃).

Table S1 The ROP of *rac*-LA catalyzed by complexes **1a**–**5a** and **1b**–**4b** at 100 ˚C and 110˚C[a]

Entry	Complex	[*rac*-LA]:[Al]:[BnOH]	T (˚C)	Time (h)	Conv.[b] (%)	$M_{n,calc}$[c] (10^4)	$M_{n,GPC}$[d] (10^4)	PDI[e]	P_m[f]
1	**1a**	100:1:1	100	2	98	1.42	0.98	1.29	0.67
2	**1a**	100:1:1	110	1	98	1.42	0.96	1.34	0.68
3	**2a**	100:1:1	100	2	97	1.41	0.89	1.28	0.68
4	**2a**	100:1:1	110	1	96	1.44	0.68	1.43	0.67
5	**3a**	100:1:1	100	2	98	1.42	0.95	1.29	0.68
6	**3a**	100:1:1	110	1	97	1.42	0.89	1.27	0.68
7	**4a**	100:1:1	100	6(2)	95(86)	1.38	0.71	1.18	0.69
8	**4a**	100:1:1	110	4(2)	96(93)	1.39	0.77	1.24	0.71
9	**5a**	100:1:1	100	2	99	1.44	1.02	1.25	0.69
10	**5a**	100:1:1	110	1	98	1.42	0.93	1.45	0.68
11	**1b**	100:1:1	100	10(2)	80(51)	1.16	0.54	1.06	0.71

12	**1b**	100:1:1	110	8(2)	93(71)	1.35	0.63	1.12	0.71
13	**2b**	100:1:1	100	4(2)	98(63)	1.42	0.84	1.22	0.73
14	**2b**	100:1:1	110	4(2)	92(85)	1.37	0.74	1.13	0.75
15	**3b**	100:1:1	100	4(2)	99(68)	1.44	1.01	1.26	0.72
16	**3b**	100:1:1	110	4(2)	95(90)	1.38	0.69	1.24	0.71
17	**4b**	100:1:1	100	10(2)	48(20)	0.70	0.41	1.11	0.72
18	**4b**	100:1:1	110	8(2)	52(38)	0.76	0.44	1.15	0.71

[a] Unless otherwise specified, the polymerizations were carried out in toluene. [b] Determined by ^{1}H NMR spectroscopy. [c] $M_{n,calc}$ = 144.13 × ([*rac*-LA]$_0$/[BnOH]$_0$) × conv. (%) + 108.13. [d] Obtained from GPC analysis in THF using polystyrene standards and multiplied by 0.58. [e] Obtained from GPC analysis. [f] Measured by homodecoupling ^{1}H NMR spectroscopy at 25 °C.

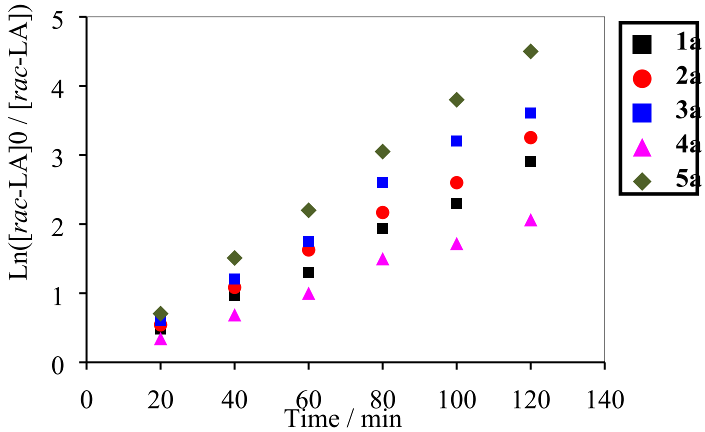

Figure S11 Relationship between ln([*rac*-LA]$_0$/[*rac*-LA]) and time of the polymerization initiated by **1a**–**5a** in the presence of BnOH in toluene at 100 °C with a ratio of [*rac*-LA]$_0$:[Al]$_0$:[BnOH]$_0$ = 100:1:1 ([*rac*-LA]$_0$ = 1 M).

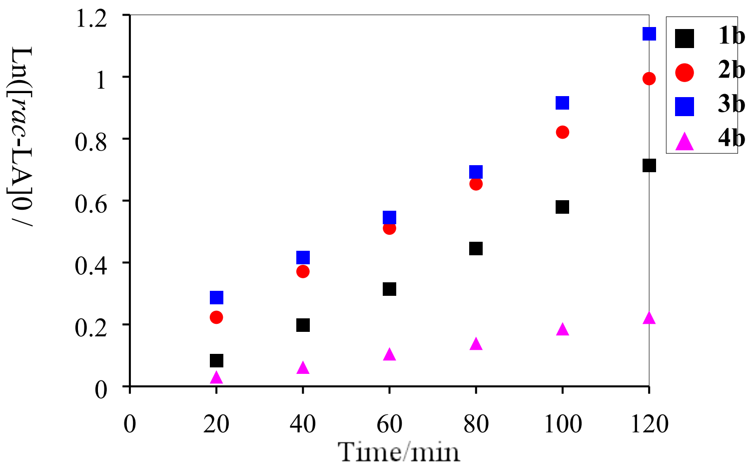

Figure S12 Relationship between ln([*rac*-LA]$_0$/[*rac*-LA]) and time of the polymerization initiated by **1b**–**4b** in the presence of BnOH in toluene at 100 °C with a ratio of [*rac*-LA]$_0$:[Al]$_0$:[BnOH]$_0$ = 100:1:1 ([*rac*-LA]$_0$ = 1 M).

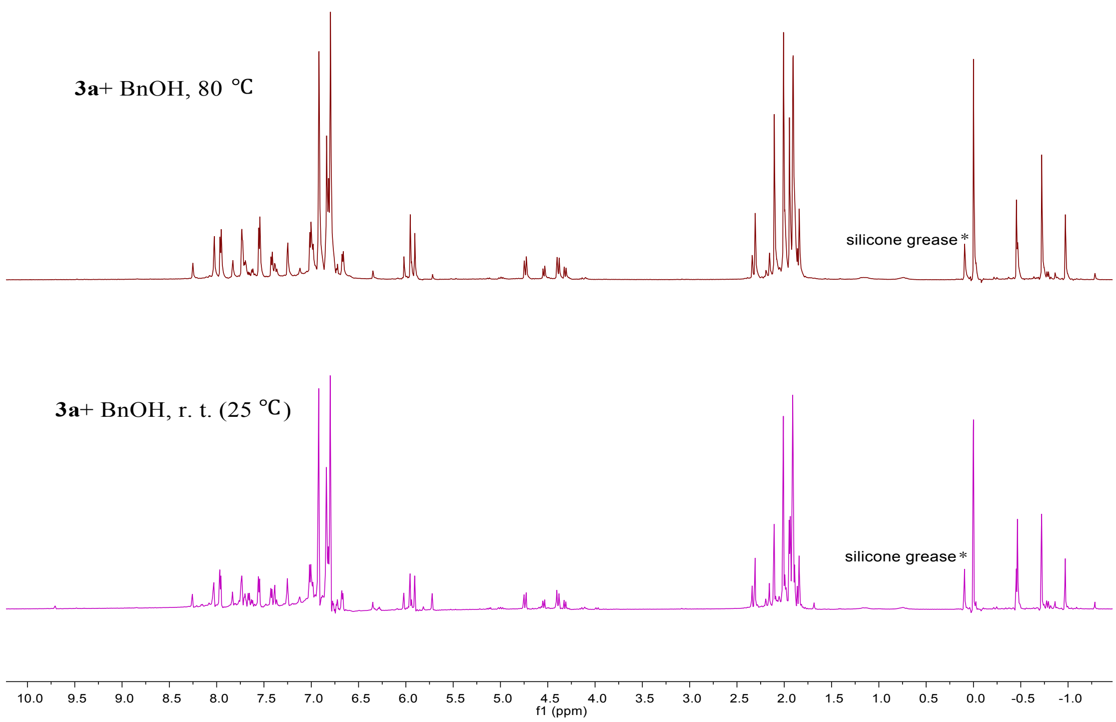

Figure S13 The ^{1}H NMR spectra of complexes **3a** with BnOH (600 MHz, C_7D_8)

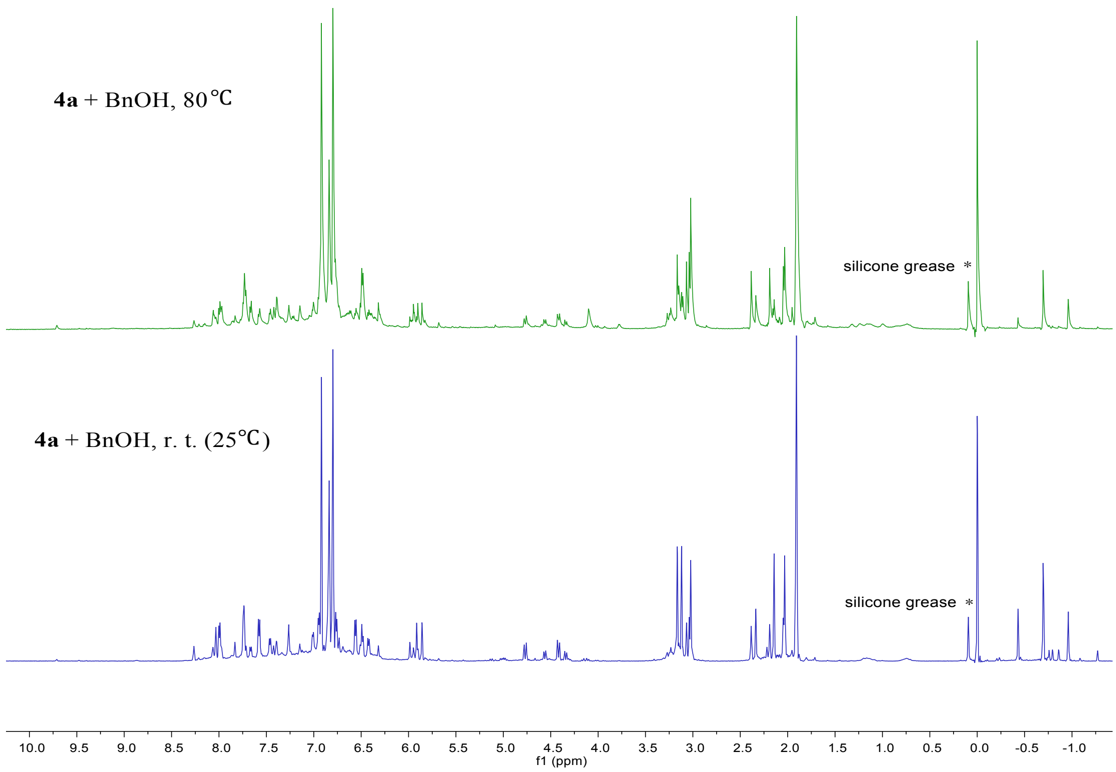

Figure S14 The ^{1}H NMR spectra of complexes **4a** with BnOH (600 MHz, C_7D_8)

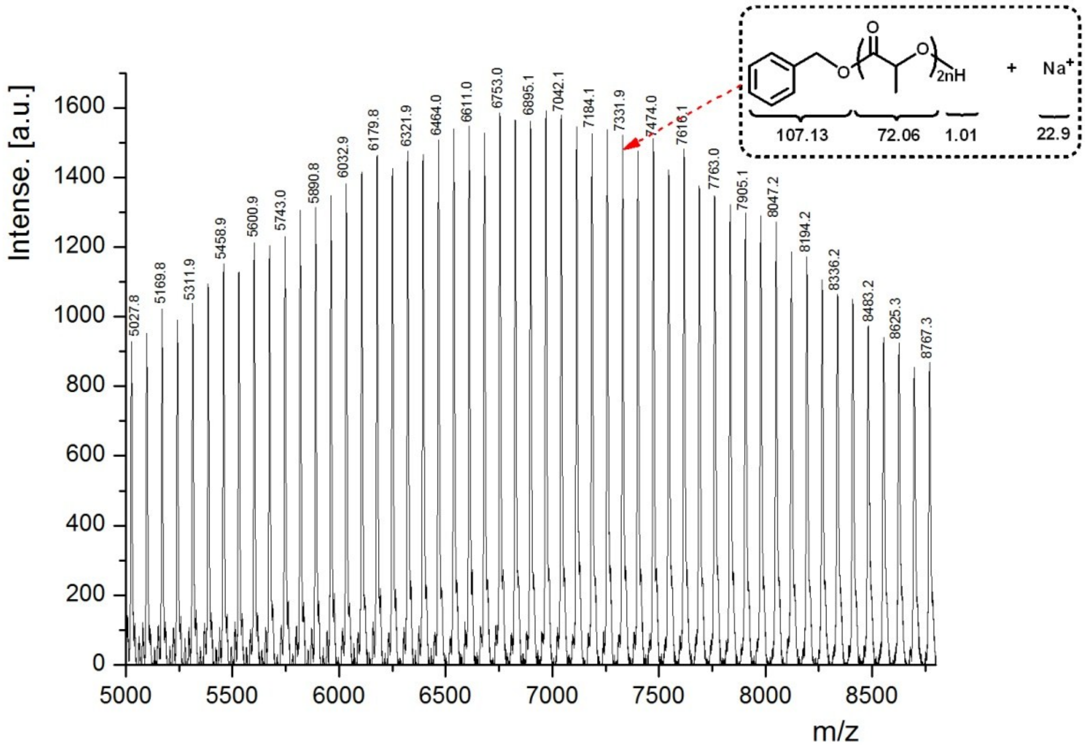

Figure S15 MALDI-TOF MS analysis for the resulting PLA produced by **2a** ([*rac*-LA]$_0$:[Al]$_0$:[BnOH]$_0$ = 100:1:1, 80 ℃).

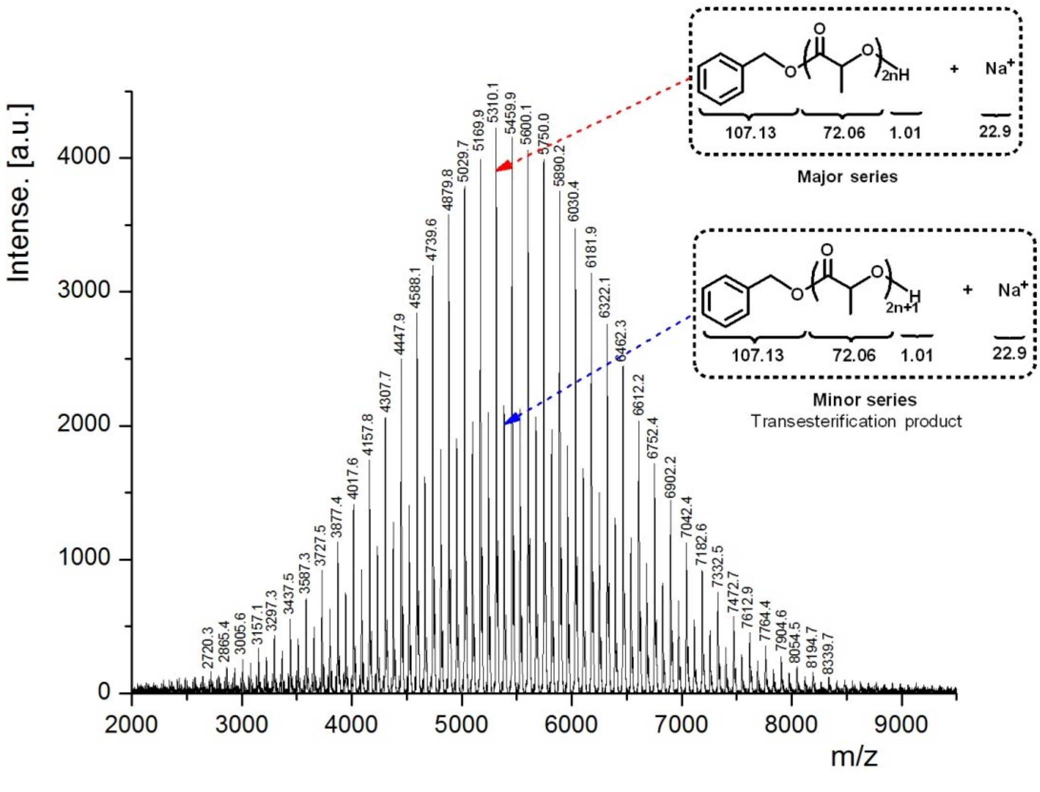

Figure S16 MALDI-TOF MS analysis for the resulting PLA produced by **2b** ([*rac*-LA]$_0$: Al]$_0$:[BnOH]$_0$ = 100:1:1, 80 ℃).

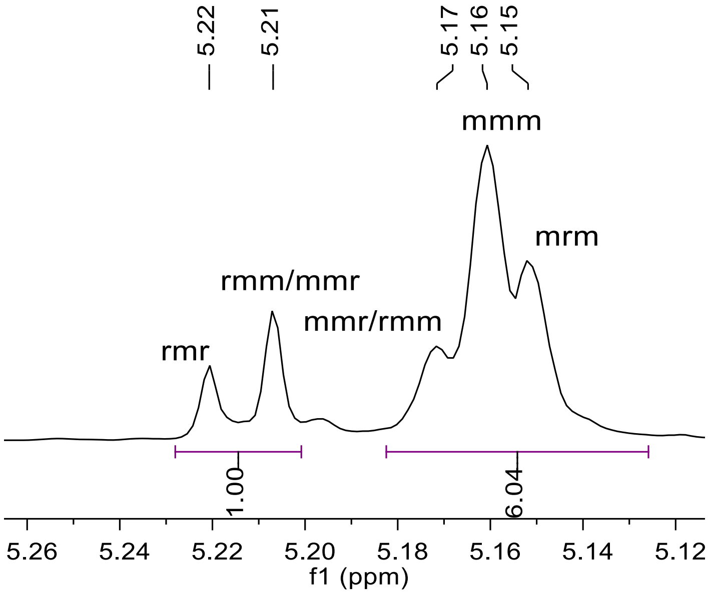

Figure S17 Methine region spectrum of homonuclear decoupled [1]H NMR spectrum ($CDCl_3$, 25 ºC, 600 MHz, $P_m = 0.72$, Table 5, entry 2)

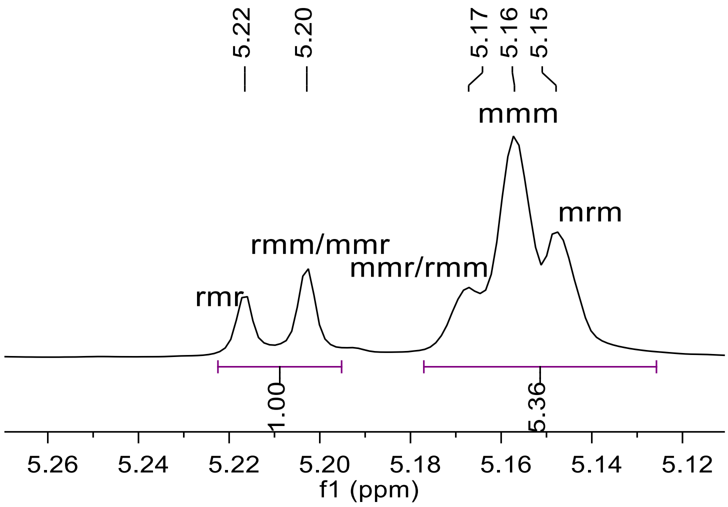

Figure S18 Methine region spectrum of homonuclear decoupled [1]H NMR spectrum ($CDCl_3$, 25 ºC, 600 MHz, $P_m = 0.69$, Table 5, entry 3)

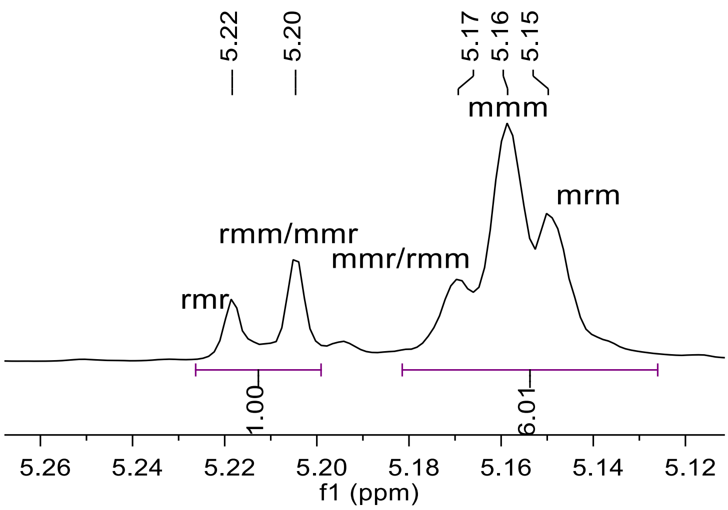

Figure S19 Methine region spectrum of homonuclear decoupled [1]H NMR spectrum ($CDCl_3$, 25 ºC, 600 MHz, P_m = 0.71, Table 5, entry 4)

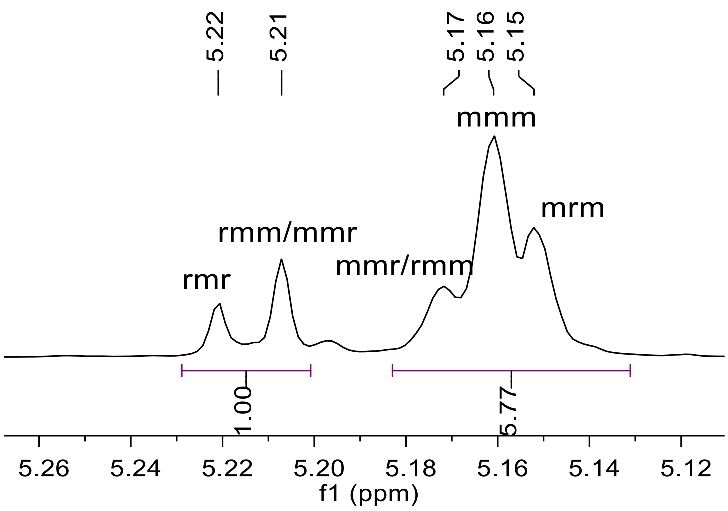

Figure S20 Methine region spectrum of homonuclear decoupled [1]H NMR spectrum ($CDCl_3$, 25 ºC, 600 MHz, P_m = 0.70, Table 5, entry 5)

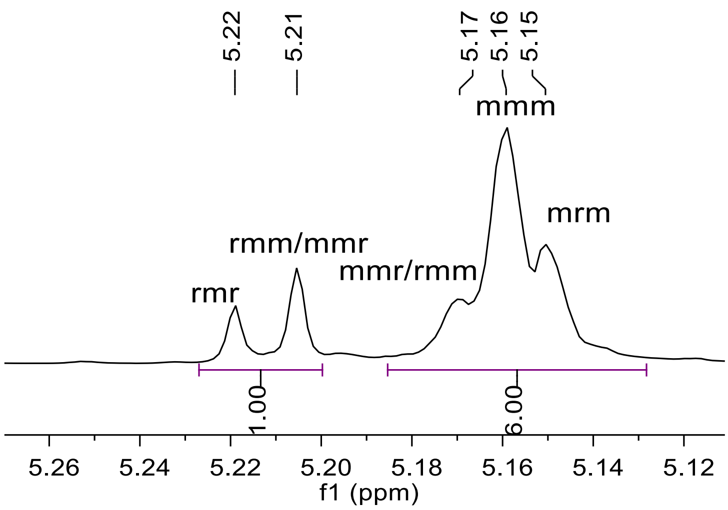

Figure S21 Methine region spectrum of homonuclear decoupled [1]H NMR spectrum ($CDCl_3$, 25 ºC, 600 MHz, $P_m = 0.71$, Table 5, entry 7)

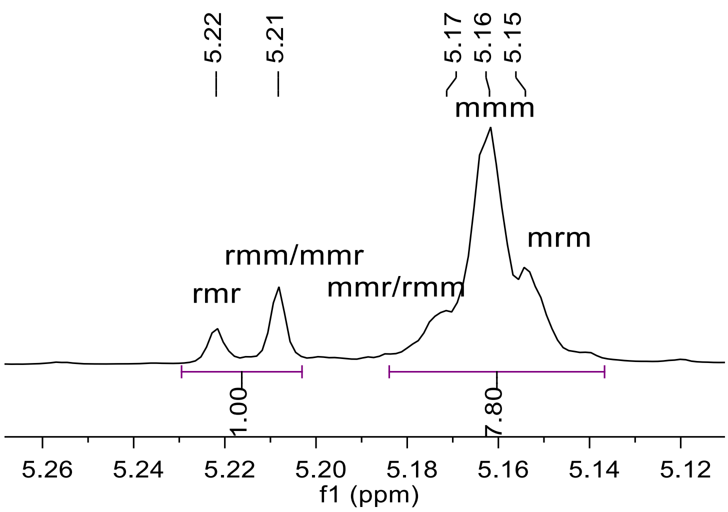

Figure S22 Methine region spectrum of homonuclear decoupled [1]H NMR spectrum ($CDCl_3$, 25 ºC, 600 MHz, $P_m = 0.77$, Table 5, entry 8)

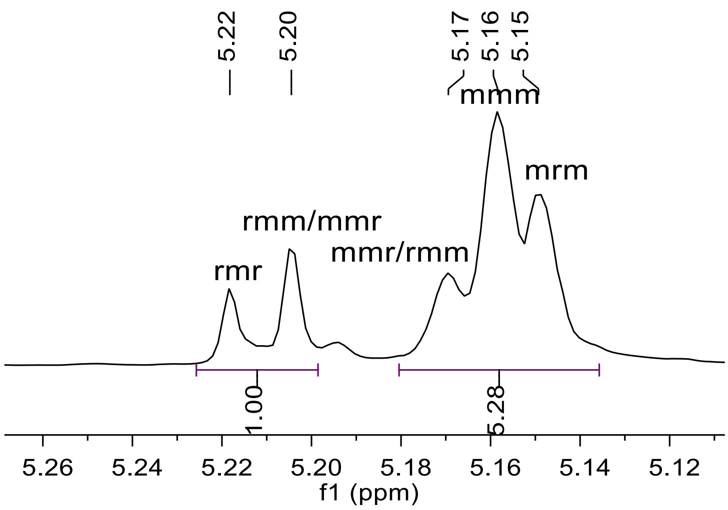

Figure S23 Methine region spectrum of homonuclear decoupled ^{1}H NMR spectrum ($CDCl_3$, 25 ºC, 600 MHz, P_m = 0.68, Table S1, entry 3)

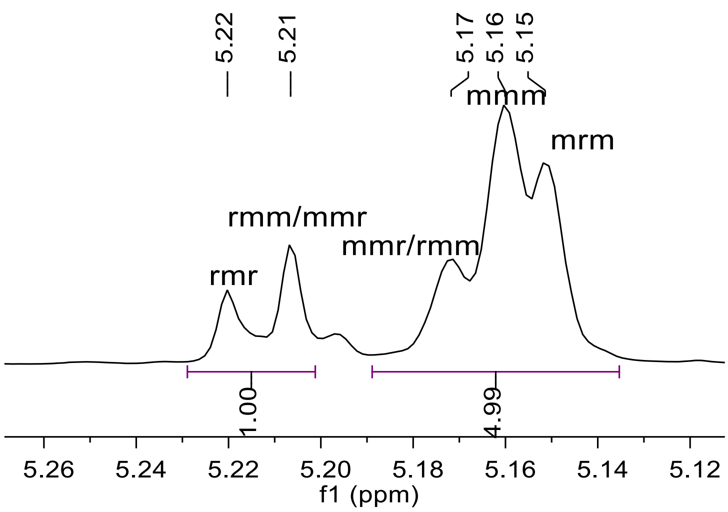

Figure S24 Methine region spectrum of homonuclear decoupled ^{1}H NMR spectrum ($CDCl_3$, 25 ºC, 600 MHz, P_m = 0.67, Table S1, entry 4)

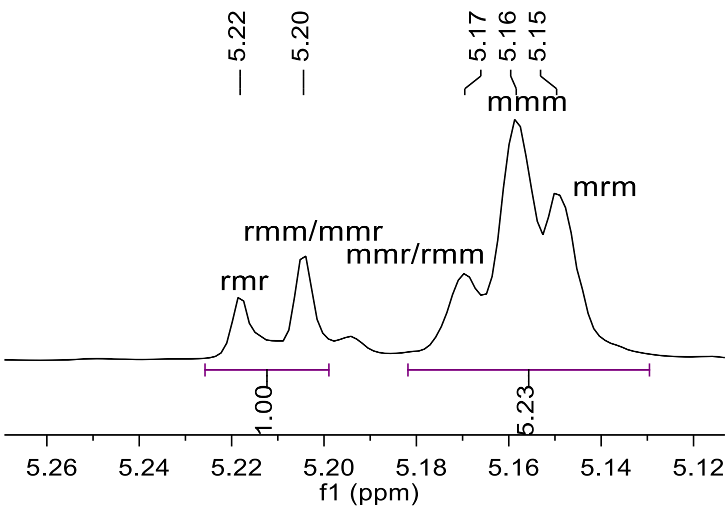

Figure S25 Methine region spectrum of homonuclear decoupled [1]H NMR spectrum ($CDCl_3$, 25 ºC, 600 MHz, $P_m = 0.68$, Table S1, entry 5)

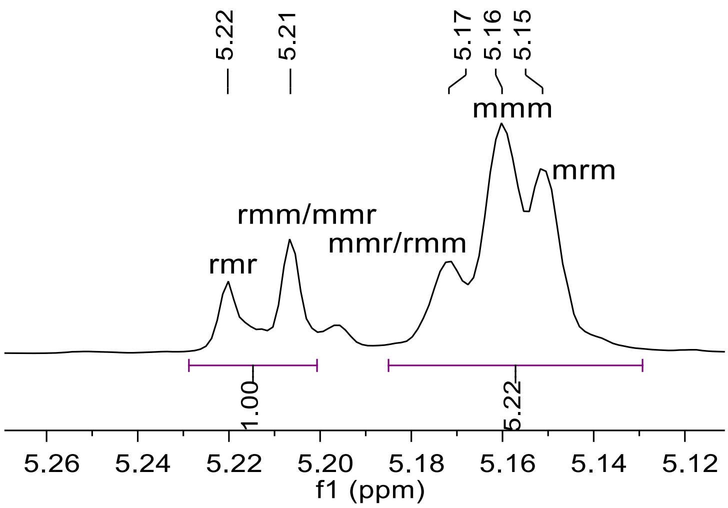

Figure S26 Methine region spectrum of homonuclear decoupled [1]H NMR spectrum ($CDCl_3$, 25 ºC, 600 MHz, $P_m = 0.68$, Table S1, entry 6)

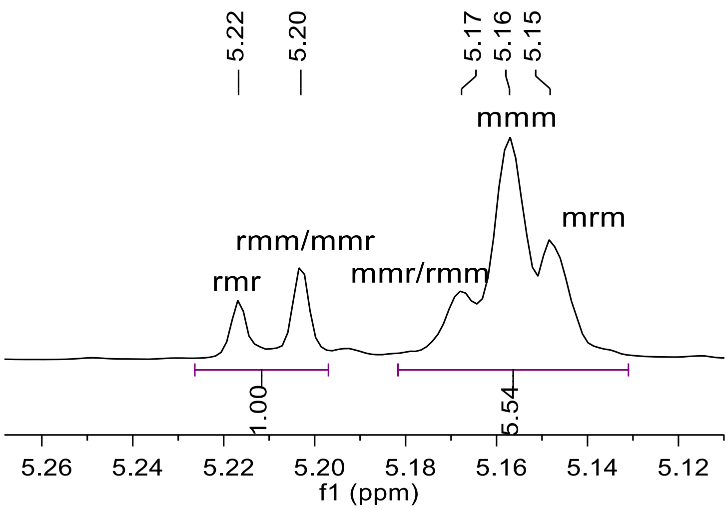

Figure S27 Methine region spectrum of homonuclear decoupled [1]H NMR spectrum ($CDCl_3$, 25 ºC, 600 MHz, $P_m = 0.69$, Table S1, entry 7)

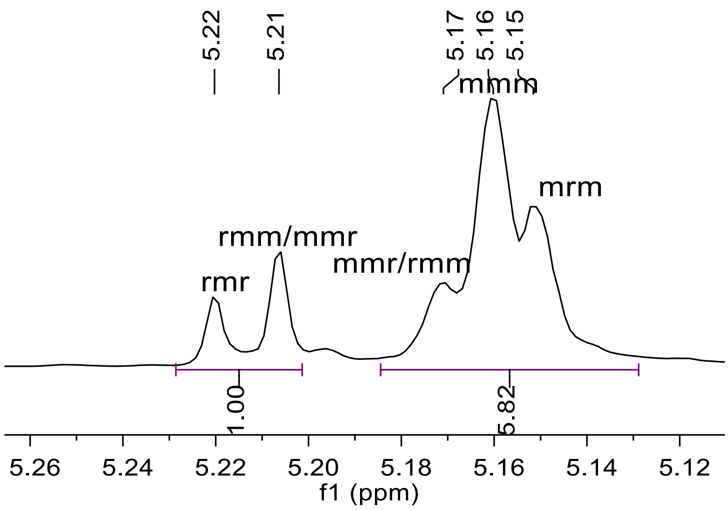

Figure S28 Methine region spectrum of homonuclear decoupled [1]H NMR spectrum ($CDCl_3$, 25 ºC, 600 MHz, $P_m = 0.71$, Table S1, entry 8)

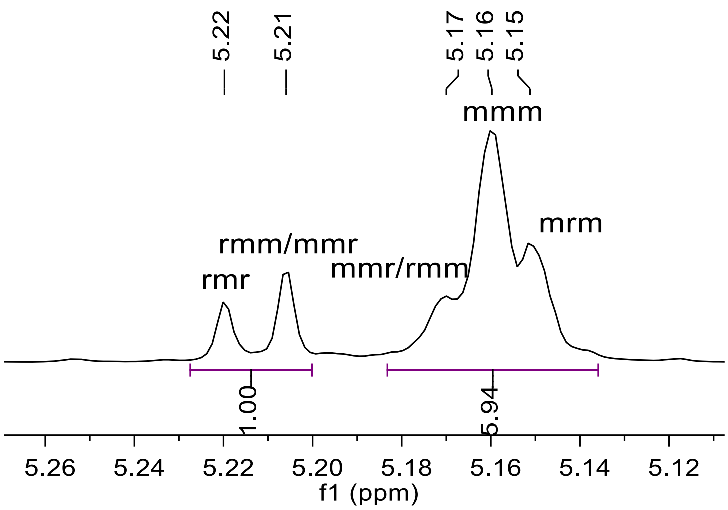

Figure S29 Methine region spectrum of homonuclear decoupled [1]H NMR spectrum ($CDCl_3$, 25 ºC, 600 MHz, $P_m = 0.71$, Table S1, entry 11)

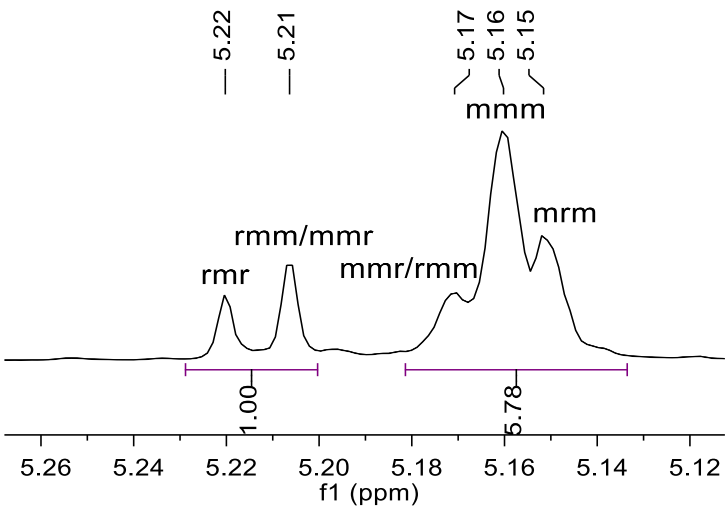

Figure S30 Methine region spectrum of homonuclear decoupled [1]H NMR spectrum ($CDCl_3$, 25 ºC, 600 MHz, $P_m = 0.71$, Table S1, entry 12)

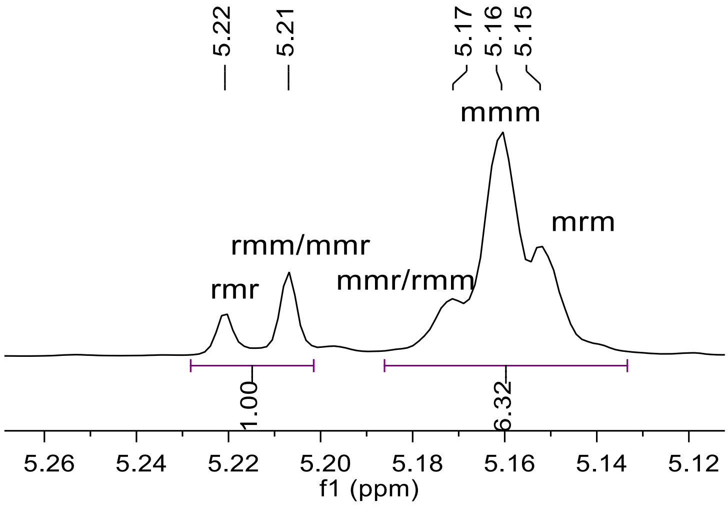

Figure S31 Methine region spectrum of homonuclear decoupled [1]H NMR spectrum ($CDCl_3$, 25 ºC, 600 MHz, $P_m = 0.73$, Table S1, entry 13)

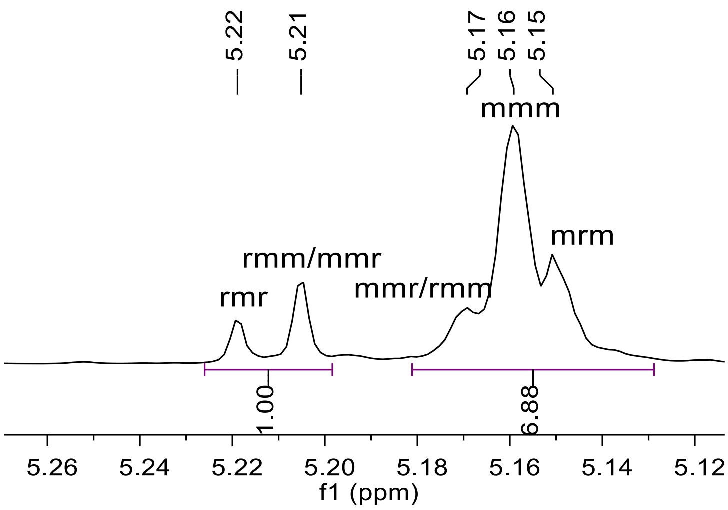

Figure S32 Methine region spectrum of homonuclear decoupled [1]H NMR spectrum ($CDCl_3$, 25 ºC, 600 MHz, $P_m = 0.75$, Table S1, entry 14)

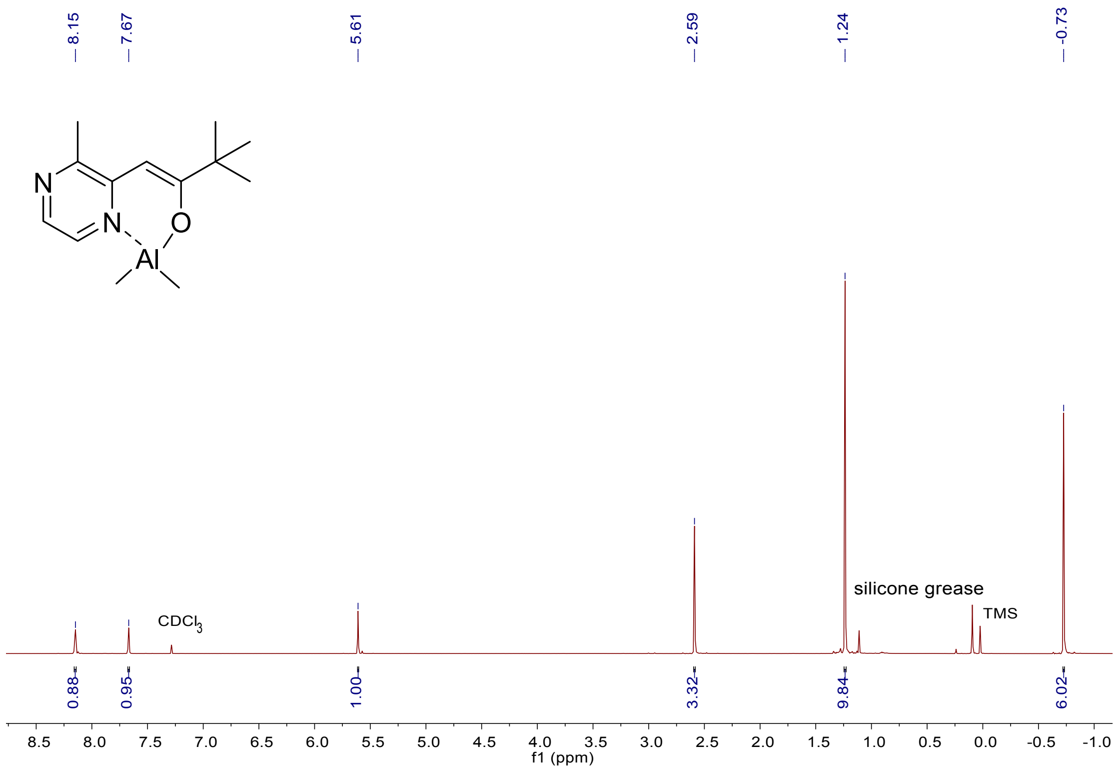

Figure S33 ^{1}H NMR spectrum of complex **1a** (600 MHz, $CDCl_3$, 25 ºC)

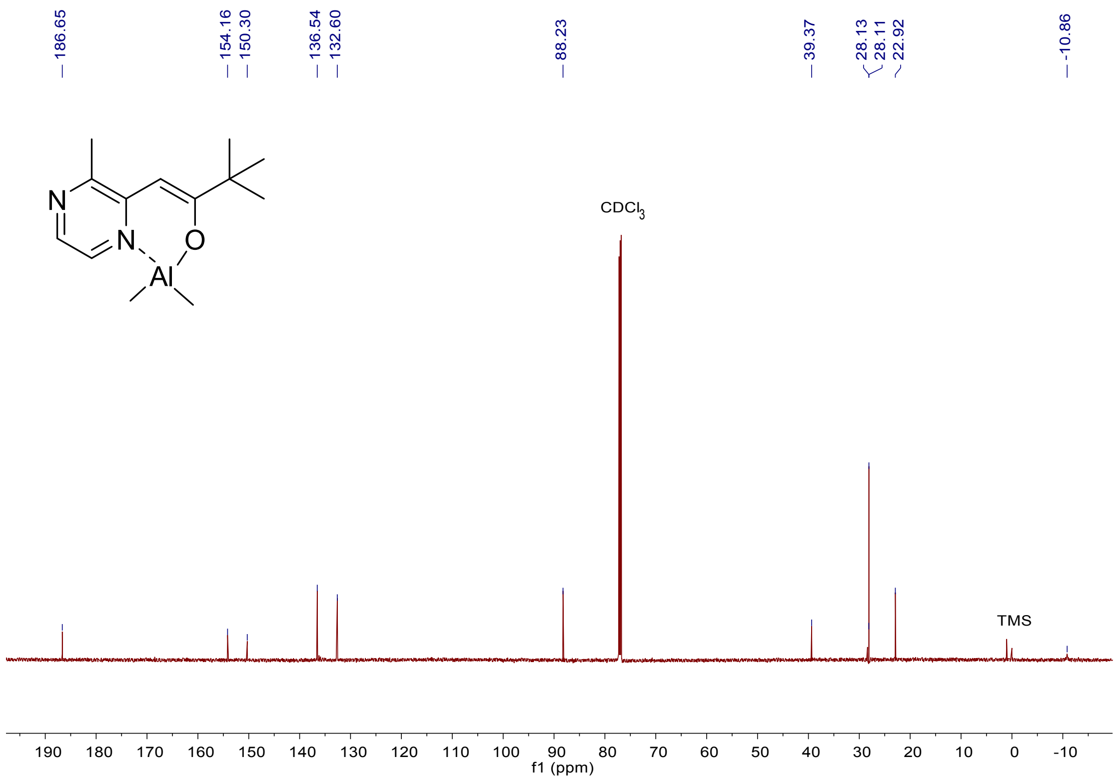

Figure S34 ^{13}C NMR spectrum of complex **1a** (151 MHz, $CDCl_3$, 25 ºC)

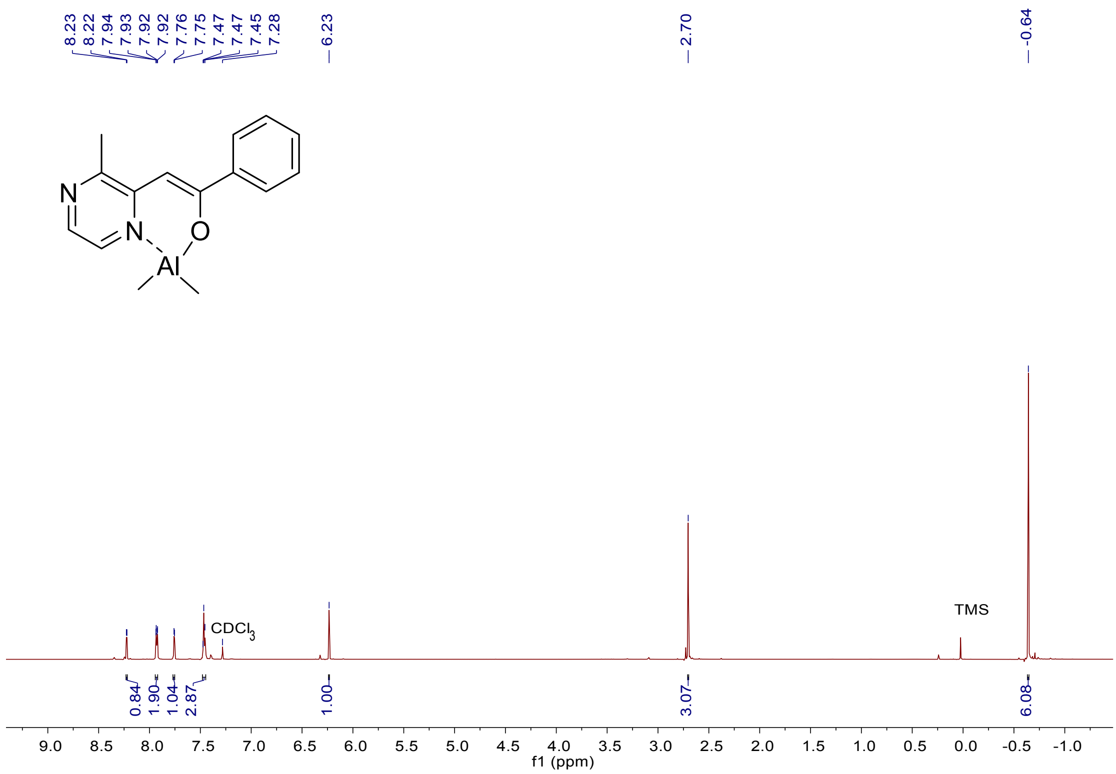

Figure S35 ^{1}H NMR spectrum of complex **2a** (600 MHz, $CDCl_3$, 25 ºC)

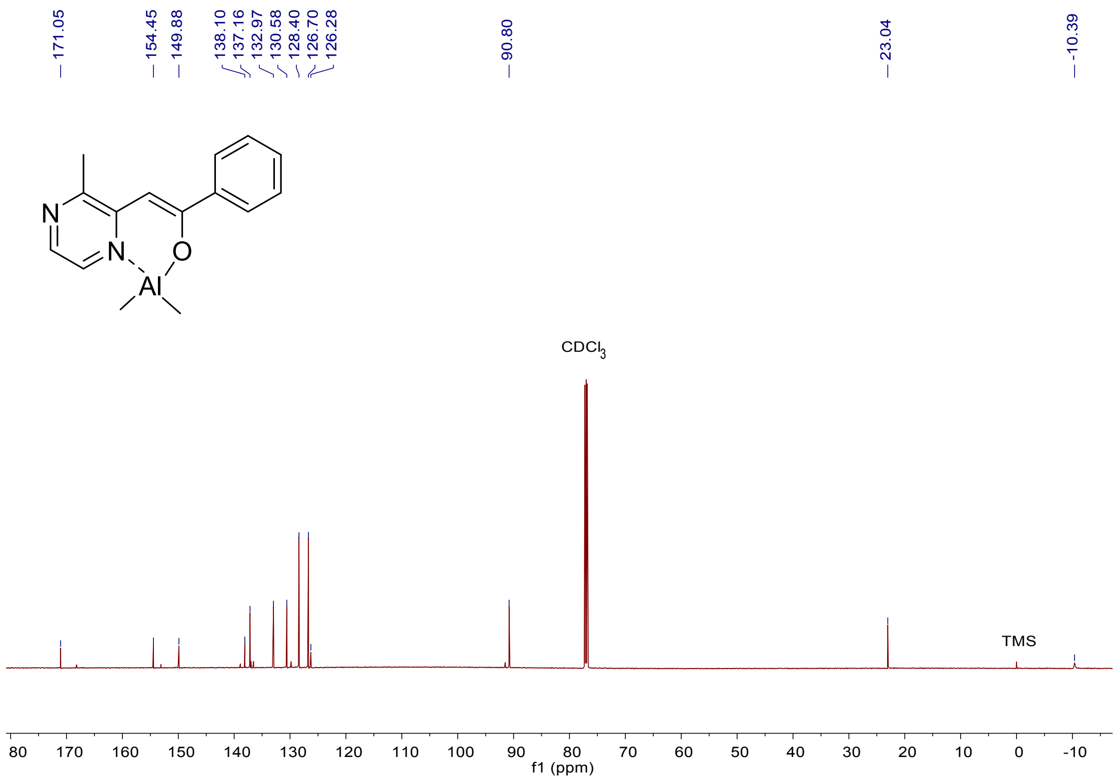

Figure S36 ^{13}C NMR spectrum of complex **2a** (151 MHz, $CDCl_3$, 25 ºC)

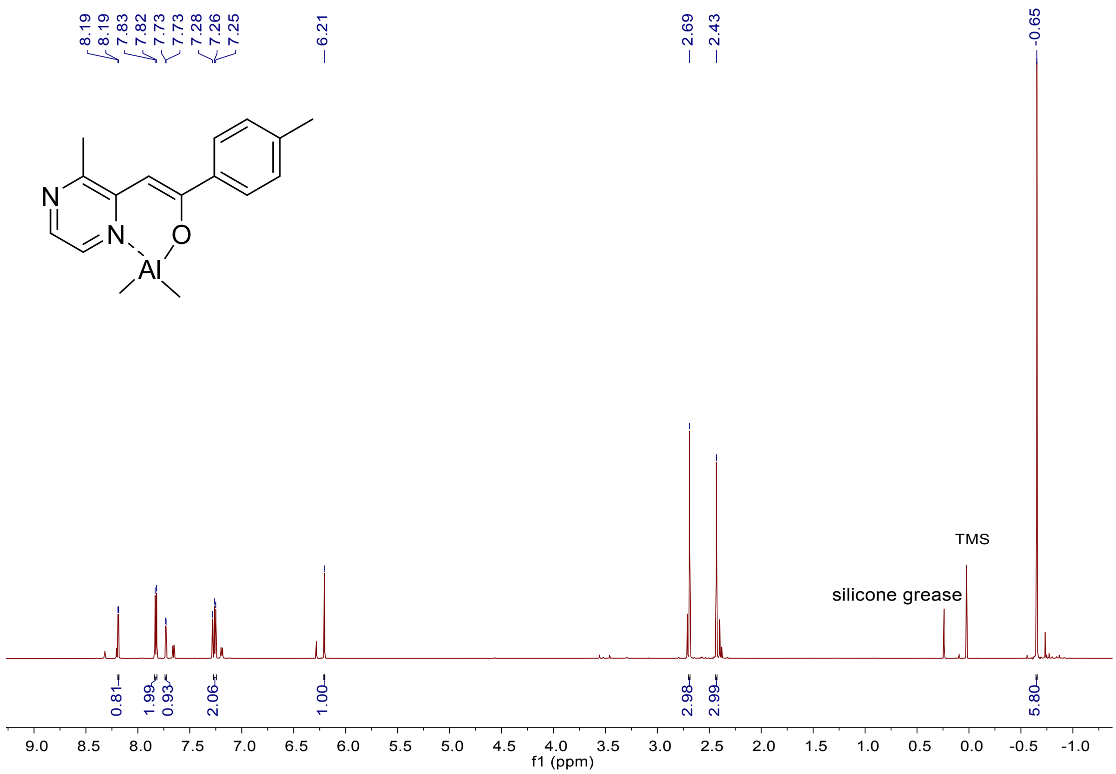

Figure S37 ^{1}H NMR spectrum of complex **3a** (600 MHz, $CDCl_3$, 25 ºC)

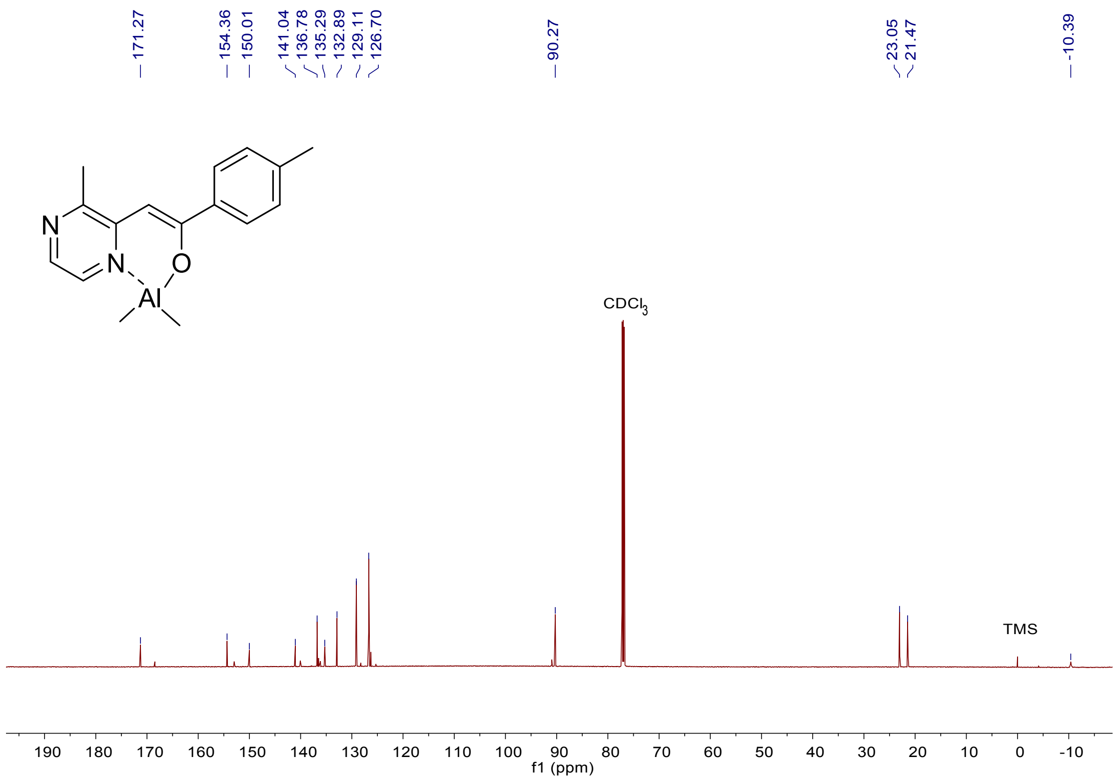

Figure S38 ^{13}C NMR spectrum of complex **3a** (151 MHz, $CDCl_3$, 25 ºC)

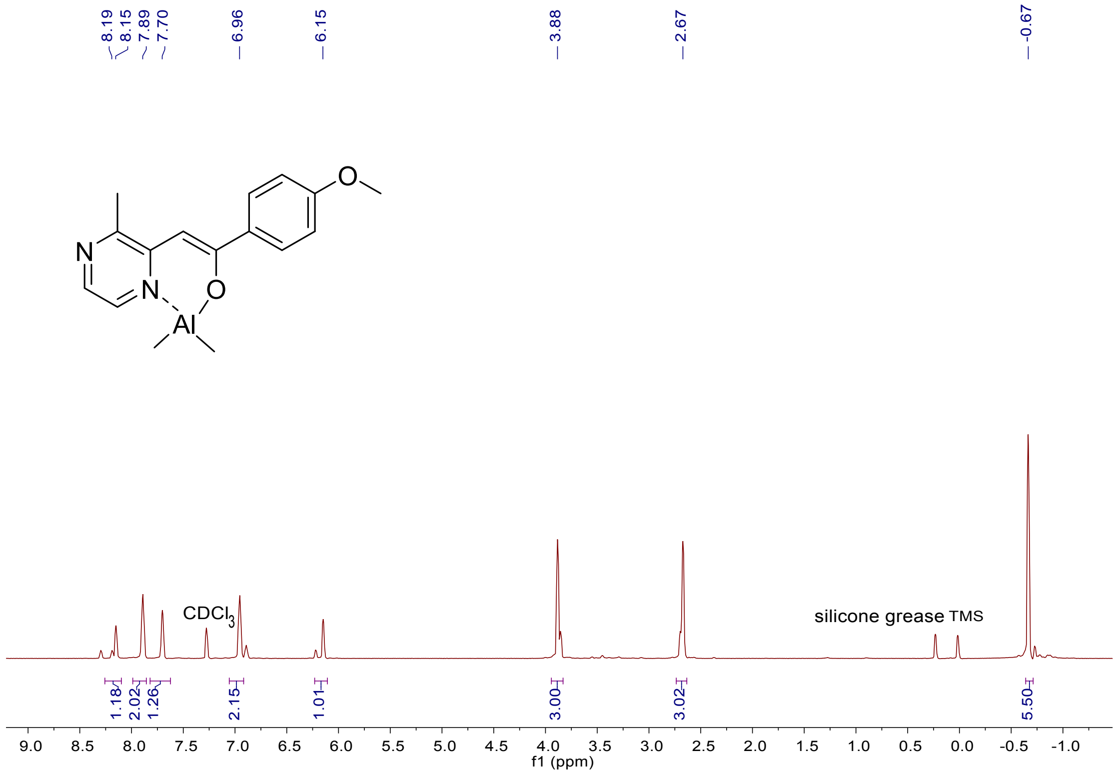

Figure S39 ^{1}H NMR spectrum of complex **4a** (600 MHz, $CDCl_3$, 25 ºC)

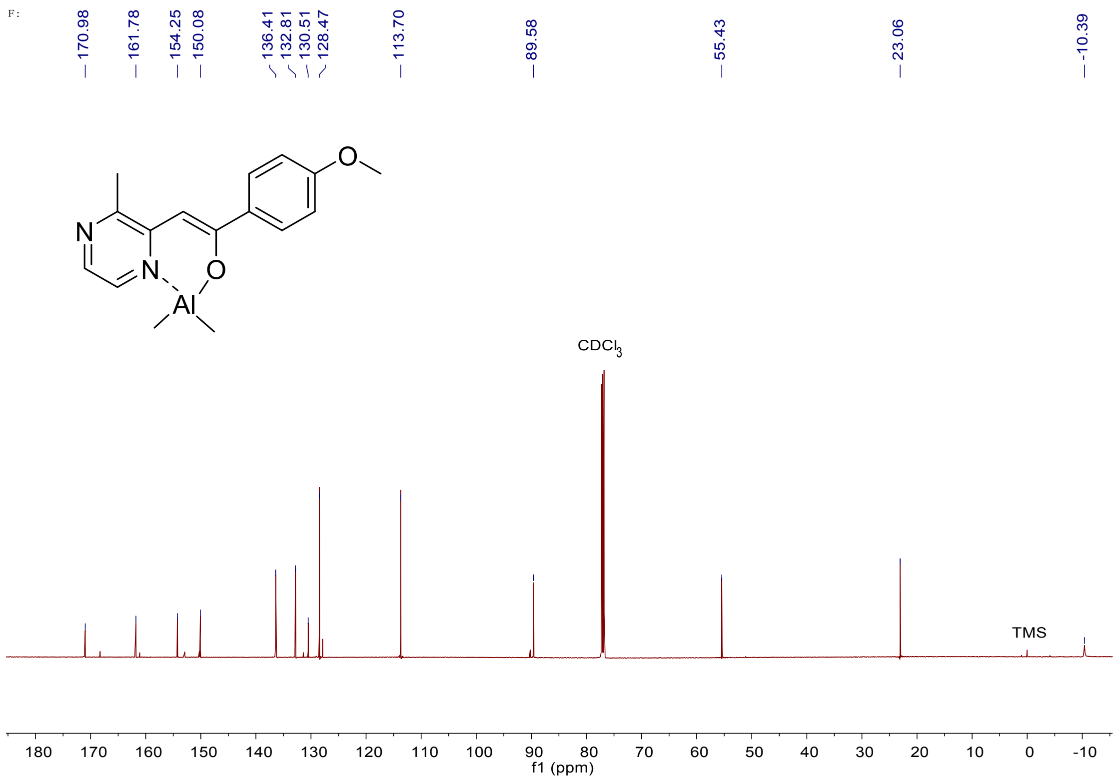

Figure S40 ^{13}C NMR spectrum of complex **4a** (151 MHz, $CDCl_3$, 25 ºC)

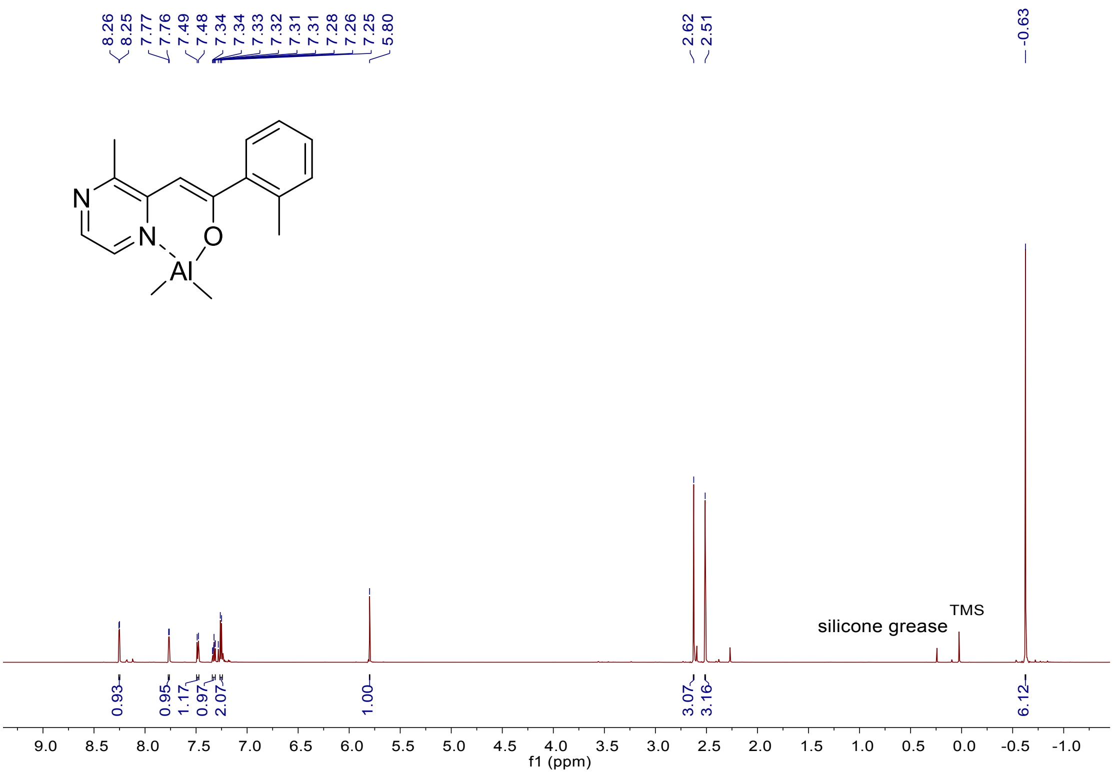

Figure S41 ^{1}H NMR spectrum of complex **5a** (600 MHz, $CDCl_3$, 25 ºC)

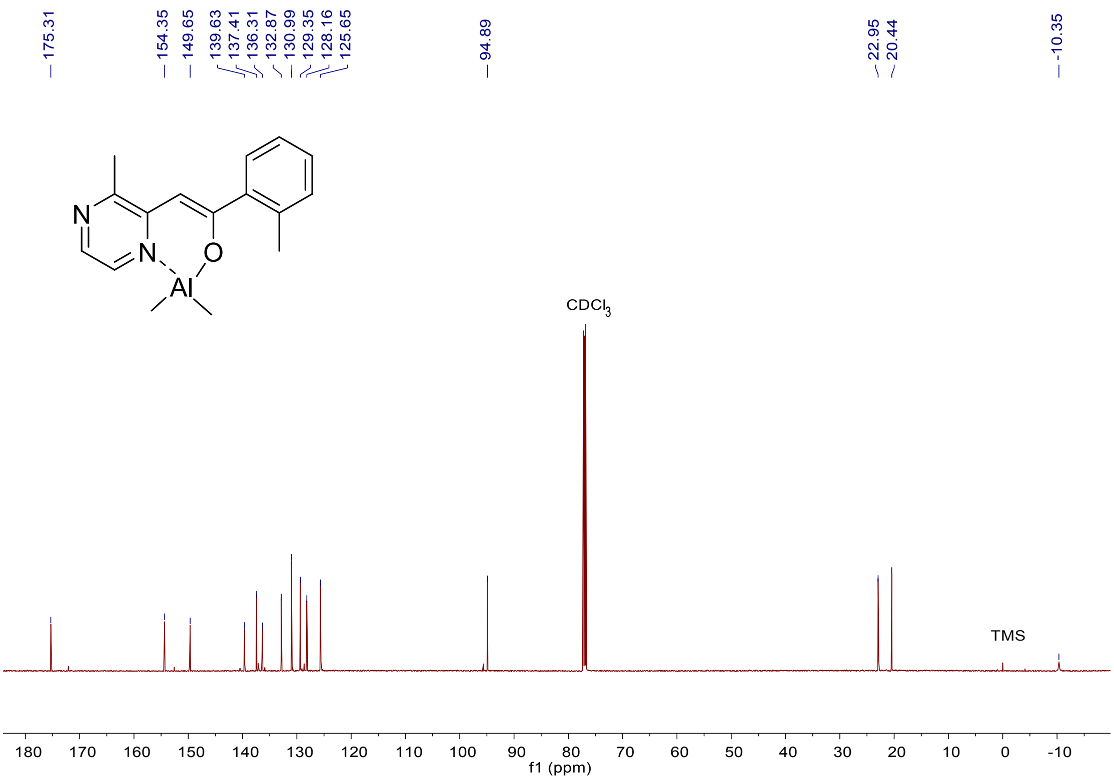

Figure S42 ^{13}C NMR spectrum of complex **5a** (151 MHz, $CDCl_3$, 25 ºC)

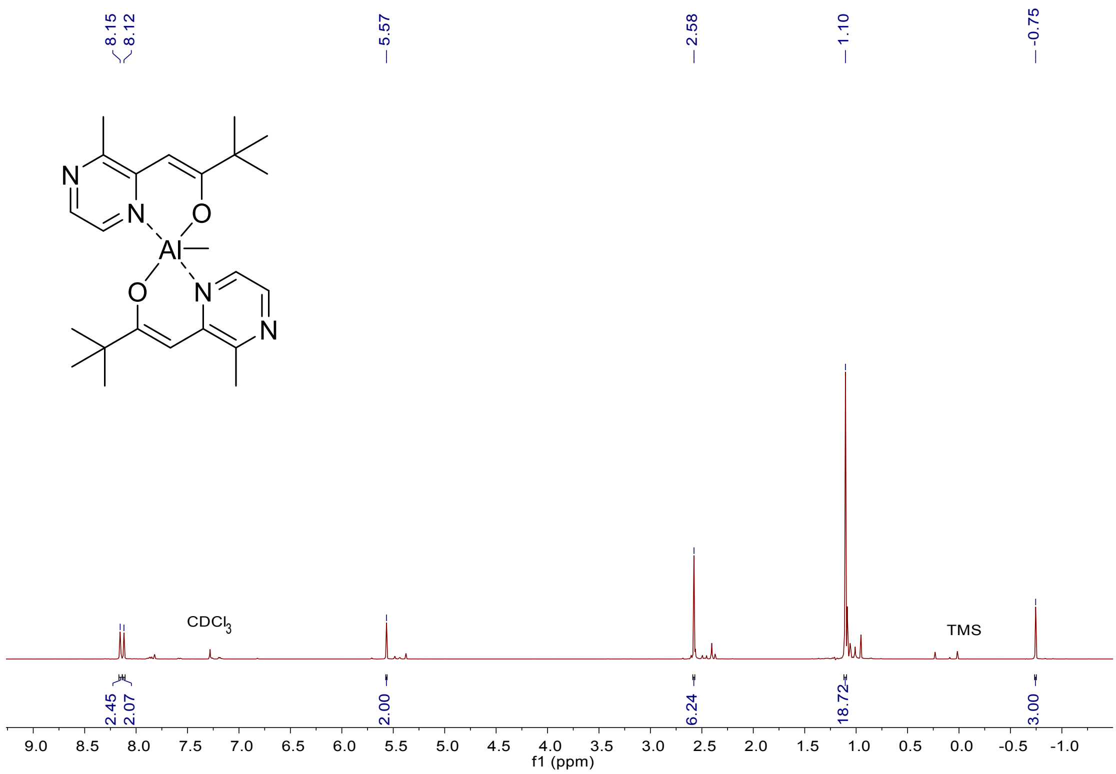

Figure S43 ^{1}H NMR spectrum of complex **1b** (600 MHz, $CDCl_3$, 25 ºC)

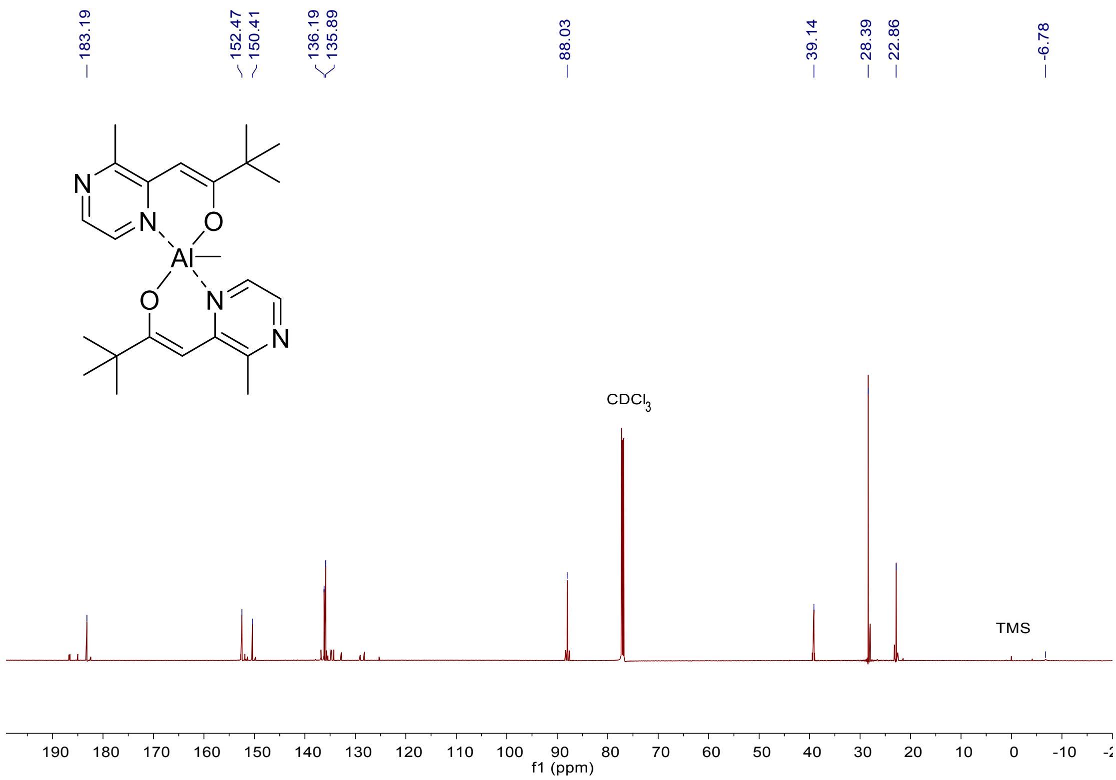

Figure S44 ^{13}C NMR spectrum of complex **1b** (151 MHz, $CDCl_3$, 25 ºC)

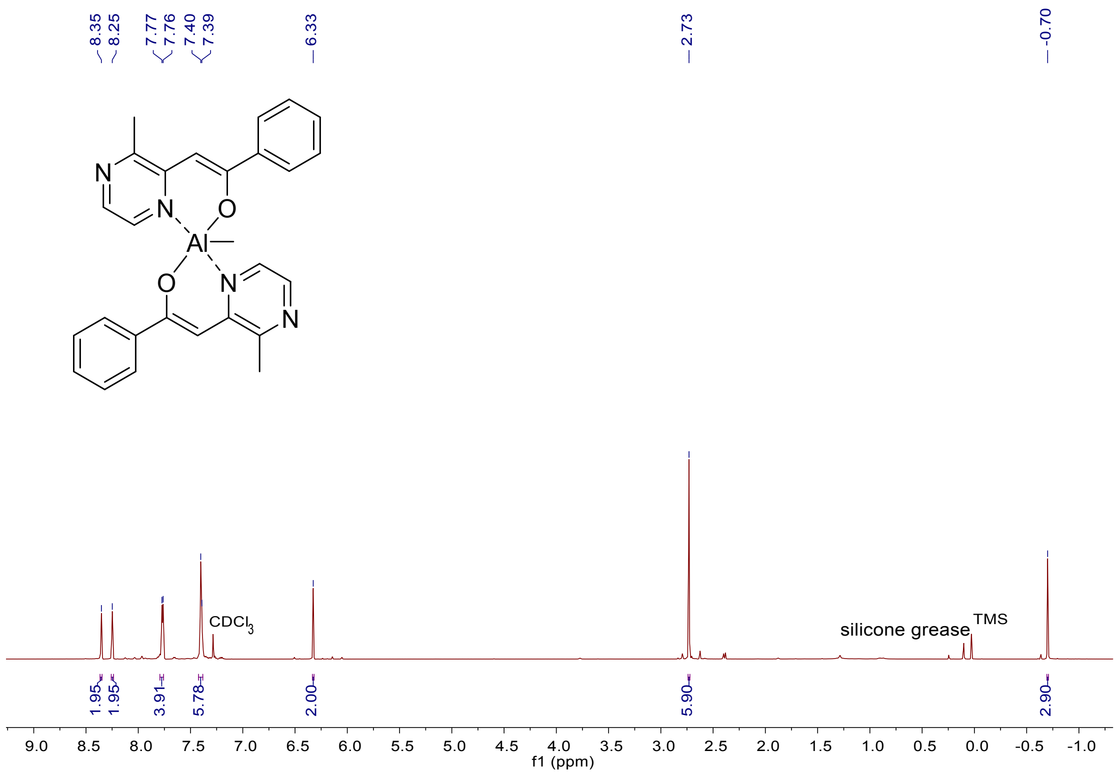

Figure S45 ^{1}H NMR spectrum of complex **2b** (600 MHz, $CDCl_3$, 25 ºC)

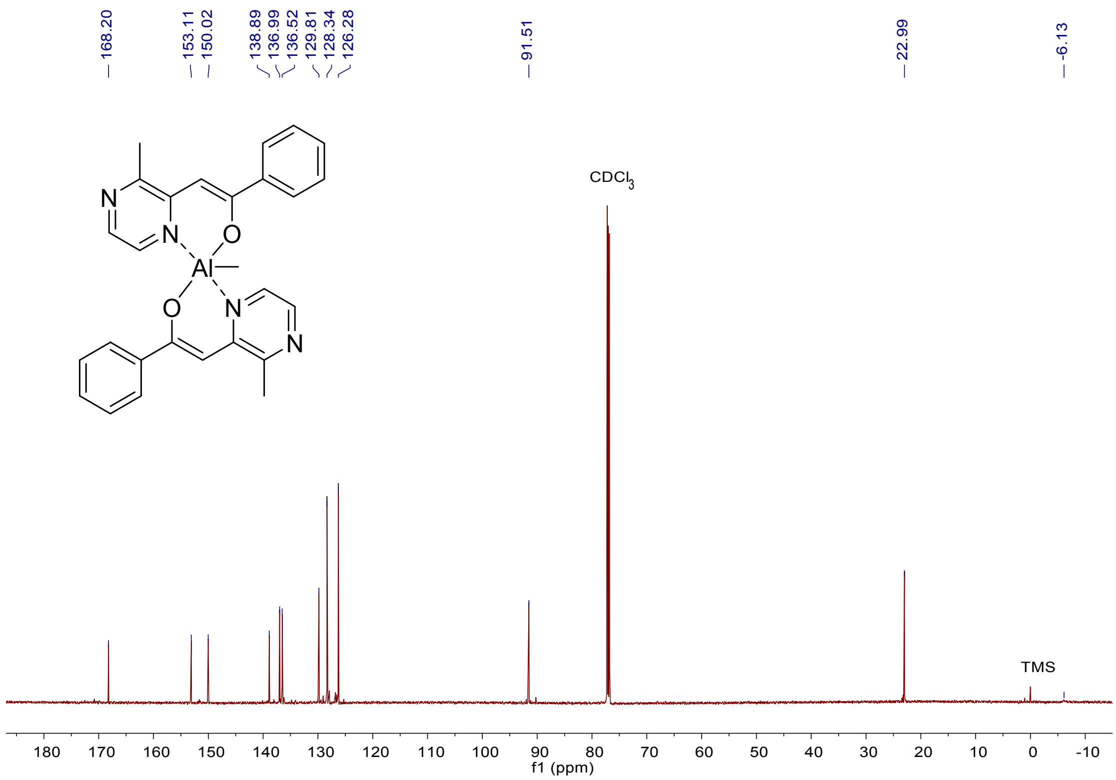

Figure S46 ^{13}C NMR spectrum of complex **2b** (151 MHz, $CDCl_3$, 25 ºC)

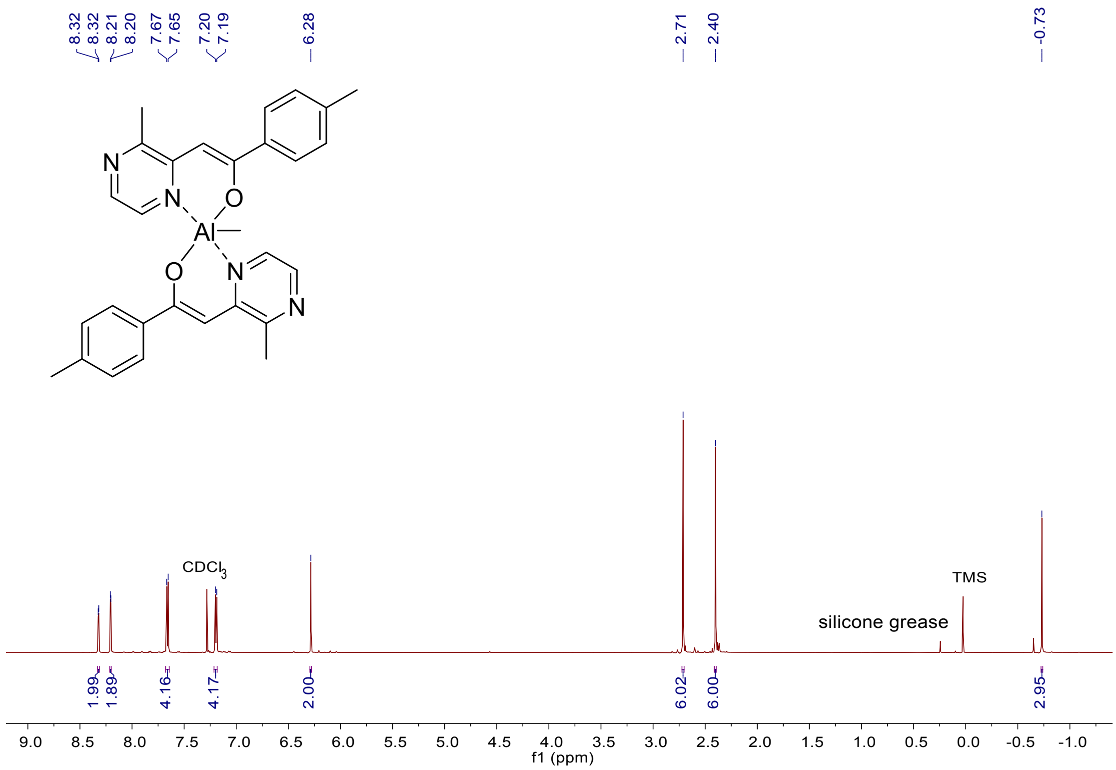

Figure S47 ^{1}H NMR spectrum of complex **3b** (600 MHz, $CDCl_3$, 25 ºC)

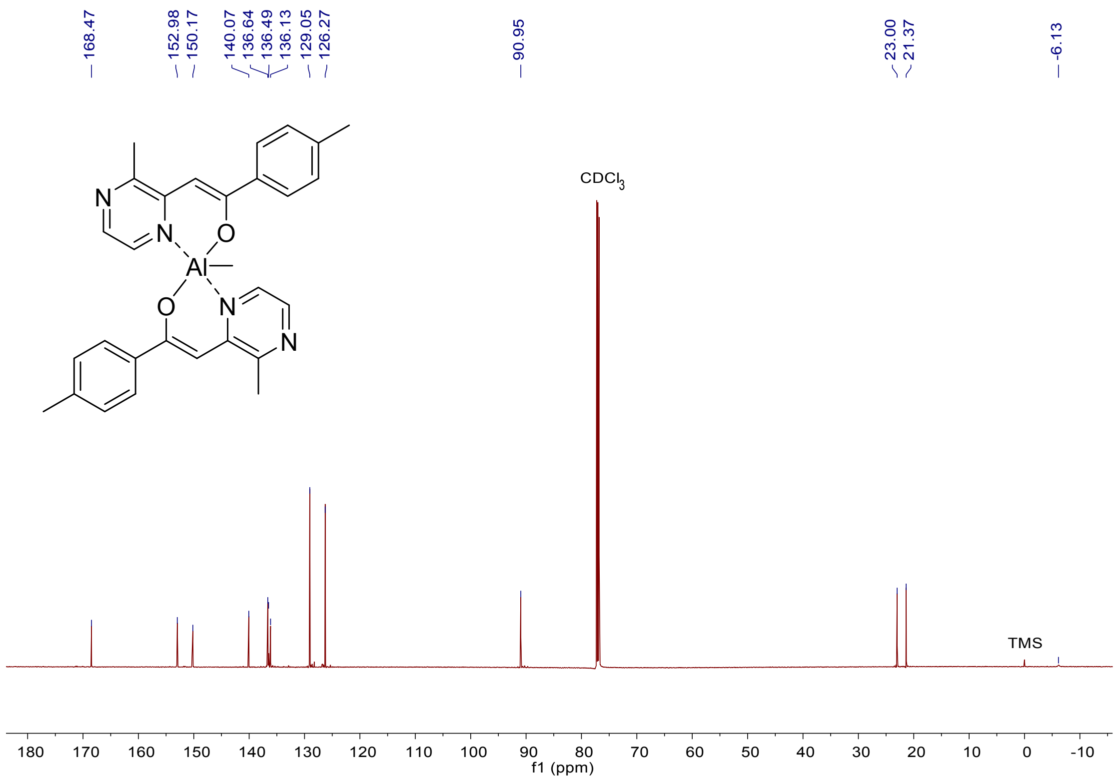

Figure S48 ^{13}C NMR spectrum of complex **3b** (151 MHz, $CDCl_3$, 25 ºC)

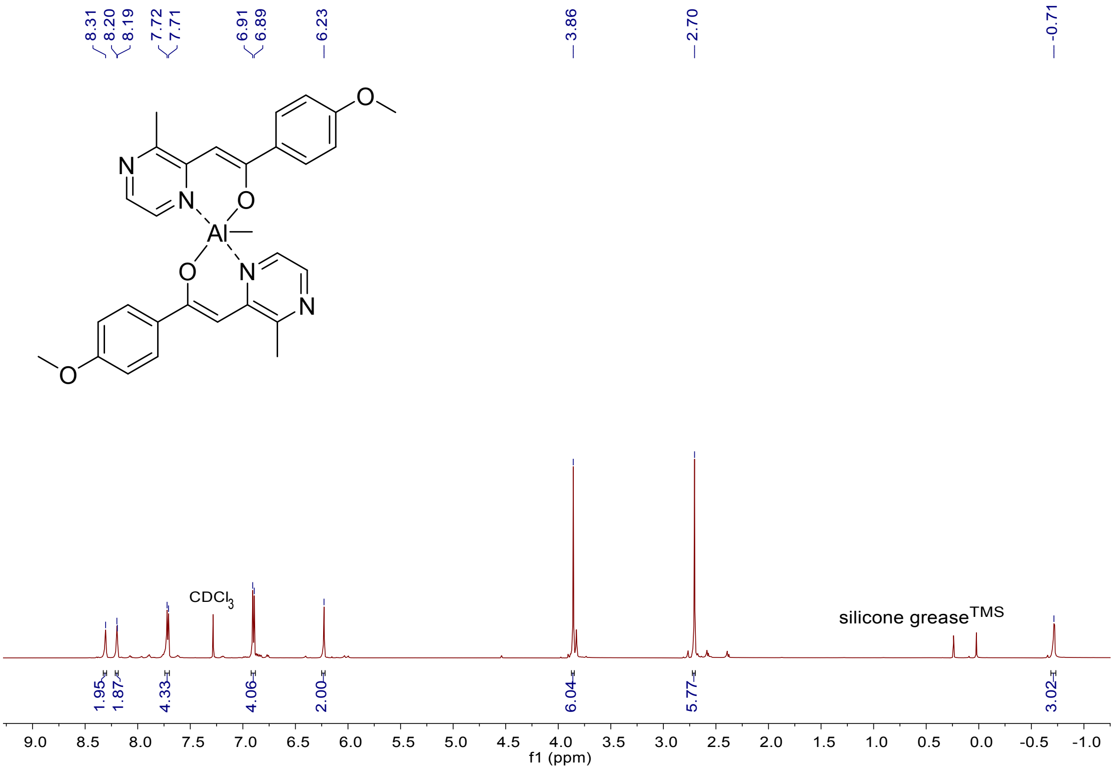

Figure S49 ^{1}H NMR spectrum of complex **4b** (600 MHz, $CDCl_3$, 25 ºC)

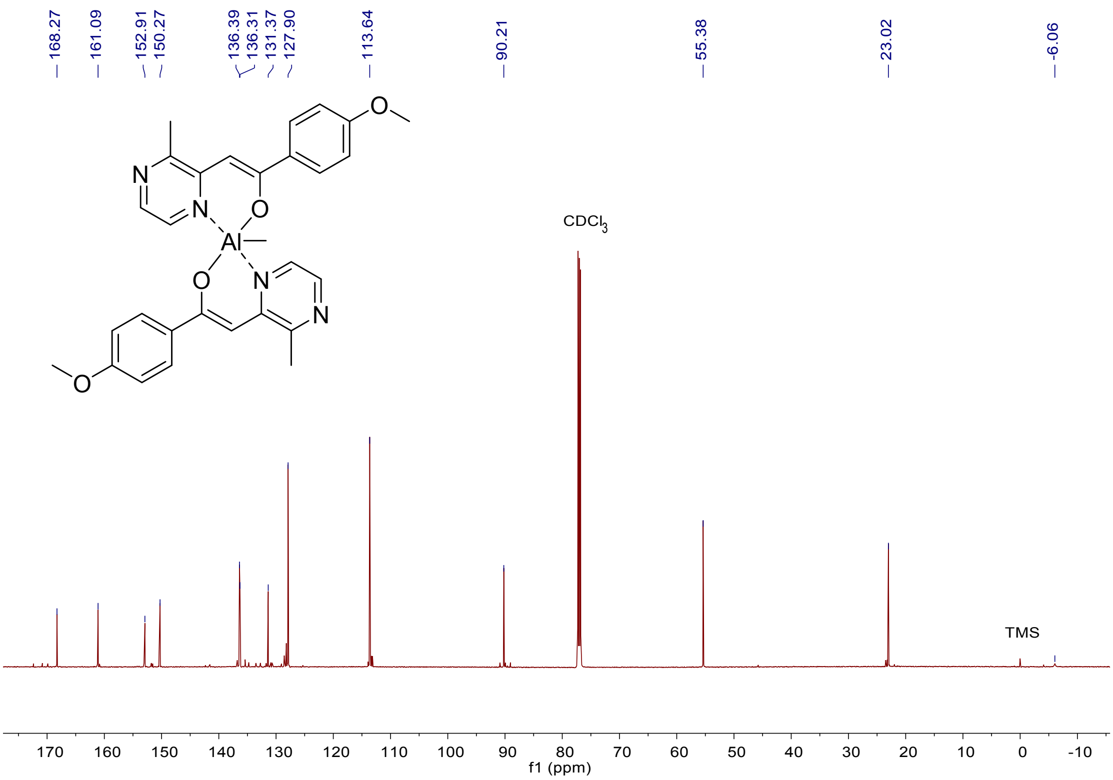

Figure S50 ^{13}C NMR spectrum of complex **4b** (151 MHz, $CDCl_3$, 25 ºC)

Table S2 Crystallographic Data for Complexes **1a-5a** and **1b**

Complex	**1a**	**2a**	**3a**	**4a**	**5a**	**1b**
Formula	$C_{13}H_{21}AlN_2O$	$C_{15}H_{17}AlN_2O$	$C_{16}H_{19}AlN_2O$	$C_{16}H_{19}AlN_2O_2$	$C_{16}H_{19}AlN_2O$	$C_{23}H_{33}AlN_4O_2$
Formula weight	248.30	268.29	282.31	298.31	282.31	424.51
Crystal system	Monoclinic	Monoclinic	Monoclinic	triclinic	Monoclinic	triclinic
Space group	$P2_1/c$	$P2_1/c$	$P2_1/n$	P-1	$P2_1$	P-1
Colour of crystal	yellow	yellow	yellow	yellow	yellow	yellow
a(Å)	10.0772(4)	10.5229(7)	7.2328(3)	7.2633(4)	11.0638(5)	9.3482(3)
b(Å)	18.7181(7)	20.9439(13)	21.7930(10)	9.1510(5)	7.7724(3)	9.3936(3)
c(Å)	15.9632(6)	13.8001(9)	9.9600(5)	12.0875(7)	18.4728(8)	14.7919(5)
α(°)	90	90	90	92.424(2)	90	96.8420(10)
β(°)	91.6530(10)	108.341(2)	106.2000(10)	95.554(2)	106.3590(10)	98.7150(10)
γ(°)	90	90	90	95.322(2)	90	109.8230(10)
V(Å^3)	3009.8(2)	2886.9(3)	1507.60(12)	795.13(8)	1524.21(11)	1187.37(7)
Temperature (K)	200(2)	200(2)	200(2)	200(2)	200(2)	200(2)
Z	8	8	4	2	4	2
D(gcm^{-3})	1.096	1.235	1.244	1.246	1.230	1.187
μ (mm^{-1})	0.123	0.134	0.132	0.133	0.130	0.111
θ range (°)	2.971-28.260	2.897-28.2775	2.833-28.2845	3.754-25.047	3.384-25.047	2.998- 25.048
F(000)	1072	1136	600	316	600	456
Reflections collected	28140	26815	14293	9599	11193	14999
Independent reflections (R_{int})	7425 (0.0302)	7079 (0.0287)	3727 (0.0296)	2763 (0.0191)	4464 (0.0198)	4166 (0.0168)
Goodness of fit on F^2	1.008	1.014	1.036	1.083	1.012	1.054
Final R indices [$I > 2\sigma(I)$]						
R_1	0.0420	0.0470	0.0420	0.0430	0.0289	0.0370
wR_2	0.0982	0.1159	0.1172	0.1141	0.0827	0.1010
R indices (all data)						
R_1	0.0588	0.0594	0.0522	0.0461	0.0311	0.0412
wR_2	0.1092	0.1257	0.1253	0.1170	0.0850	0.1047